A Mathematical Model of Vascular Tumour Growth and Invasion

M. E. Orme and M. A. J. Chaplain

School of Mathematical Sciences,

University of Bath,

Bath BA2 7AY.

Tel: (+44) 01225 826242

FAX: (+44) 01225 826492

e-mail: meo, majc@maths.bath.ac.uk

Abstract

In this paper, we develop a model of the vascularization and subsequent growth of a solid spherical tumour. The key elements that are encapsulated in this model are the development of a central necrotic core due to the collapse of blood vessels at the centre of the tumour and a peak of tumour cells advancing towards the main blood vessels together with the regression of newly–formed capillaries. Diffusion alone cannot account for all behaviour and hence we include 'taxis' in our model, whereby the movement of the tumour cells is directed towards high blood vessel densities. This means that the growth of the tumour is accompanied by the invasion of the surrounding tissue. Invasion is closely linked to metastasis, whereby tumour cells enter the blood or lymph system and hence secondary tumours or metastases arise. In the second part of the paper, we conduct a travelling wave analysis on a simplified version of the model and obtain bounds on the parameters such that the solutions are non-negative and hence biologically relevant.

1 Introduction

Perhaps the most important feature that distinguishes a malignant tumour from a benign tumour is its ability to invade surrounding tissue. Invasion is often followed by metastasis, whereby tumour cells are spread via the blood or the lymph to other parts of the body where they form distant colonies (metastases). This results in multiple secondary tumours [1] and hence the disease cannot be cured by treating the original tumour alone, thus making any attempt at treatment very difficult as eradication of the secondary tumours often leads to damage of the normal tissue.

The onset of metastasis is necessarily preceded by the vascularization of a solid tumour nodule (e.g. carcinoma) by a process known as angiogenesis. Initially the tumour is avascular, i.e. it does not have its own blood supply. The tumour is very small at this stage (1-3mm diameter) and takes in nutrients and expels waste products by diffusion alone. However, this mechanism limits the growth of the tumour [2], [3]. As the tumour grows, demand increases and nutrients diffusing through the surface of the tumour are used up before they can reach the centre. Cells at the middle of the tumour are starved of nutrients and begin to die [4]. A necrotic core will develop and eventually there will be an equilibrium between the necrotic cells at the centre and the outer layer of proliferating cells. The tumour will become dormant and growth will stop.

The tumour can overcome this deficiency by acquiring a blood supply and it does so by inducing neighbouring blood vessels to grow towards the tumour [5], [6]. The formation of blood vessels is called angiogenesis. Angiogenesis is not unique to tumour growth and it is also evident in many pathological conditions such as diabetic retinopathy, arthritis and chronic inflammation [7], [8]. Tumour angiogenesis is initiated by the release of angiogenic factors or TAF by the tumour [9]. This stimulates the endothelial cells

(EC) in neighbouring blood vessels to migrate towards the tumour. Capillary sprouts are formed which grow in length by recruiting EC from the parent vessel [10]. Neighbouring sprouts will eventually fuse together at their tips to form loops (anastomoses). The looped vessels themselves may bud or may fuse with other loops until a complex network of vessels develop. This network will eventually penetrate the tumour and furnish it with the nutrients it requires for continued growth.

A vascularized tumour, that is, a tumour which is permeated with blood vessels, rapidly increases in mass. This enormous growth in tumour volume results in the collapse of the vasculature at the centre of the tumour and once again a necrotic core will develop surrounded by a peripheral zone of live cells or 'tumour vascular envelope' [8]. In order to support continued growth the tumour's vascular system persistently remodels itself, continuing indefinitely until the tumour is removed or killed, or until the host dies. Hence it is desirable to prevent a tumour from reaching the vascular phase of growth. The inhibition of angiogenesis may lead to the inhibition of tumour growth [11], [4], [12], [13],

In the following section we will derive a mathematical model which describes the interaction between the growing tumour mass and its vasculature. We present some numerical simulations which show this interaction for different initial conditions. In section (3) the model is slightly modified and we look for travelling wave solutions with constant speed and profile. Finally, in section (4) we make various concluding remarks.

2 The Mathematical Model

This model examines the development of the tumour vascular envelope from the onset of vascularization to the eventual invasion of the (parent) blood vessel which may consequently lead to metastasis. We assume that the tumour has successfully induced angiogenesis, that is a network of capillary vessels has just reached the tumour boundary. We do not explicitly model the concentration of TAF, though this is incorporated into the model by presuming that the TAF indirectly influences vessel proliferation.

Let $n_1(\mathbf{x}, t)$ be the tumour cell density and $n_2(\mathbf{x}, t)$ be the surface area of capillary vessels per unit volume. Conservation of mass gives us

$$\frac{\partial n_1}{\partial t} + \nabla.\mathbf{J_1} = f(n_1, n_2),$$

$$\frac{\partial n_2}{\partial t} + \nabla.\mathbf{J_2} = g(n_1, n_2),$$

where $\mathbf{J}_i,\ i = 1, 2$ is the flux and $f(n_1, n_2)$ and $g(n_1, n_2)$ are the source/sink terms respectively. We assume that there is small random motion of both tumour cells and capillary vessels which can be modelled by a diffusion term with constant diffusion coefficient, i.e. $\mathbf{J}_i = -D_i \nabla n_i,\ i = 1, 2$. Many mathematical models of prevascular tumours rely on diffusion as a mechanism for tumour growth [14], [15]. In a malignant tumour, there is clearly movement of tumour cells into the capillary mass. Indeed, the appearance of metastases is a clear indication that tumour cells have invaded the blood system [1]. We assume that tumour cells react to blood vessels in a similar manner to that of 'taxis', that is the tumour cells move up a gradient of capillary vessels. Hence the flux of tumour cells is given by

$$\mathbf{J_1} = \mathbf{J_{diffusion}} + \mathbf{J_{taxis}} = -D_1 \nabla n_1 + \chi n_1 \nabla n_2,$$

where for simplicity we assume χ is a constant.

The source/sink terms are carefully chosen to describe the particular behaviour and interaction of the tumour cells and blood vessels.

For the tumour proliferation rate, we assume that during its avascular stage the tumour has reached its maximum size and has become dormant. Folkman (1985) reports that tumour cells lying nearest to a capillary have the highest [^{3}H]thymidine labelling index and that the index decreases as the distance from the capillary increases. Hence the proliferation rate is dependent on the surface area of capillary vessels n_2. We also assume that, given an adequate supply of nutrients, the proliferation of tumour cells is potentially exponential since tumour-induced angiogenesis will continue indefinitely until the tumour is eradicated or the host dies [4]. Hence we model the tumour cell proliferation rate by rn_1n_2.

The vascular proliferation rate is assumed to be of a Michaelis-Menten form which saturates as n_2 increases, so that there is a finite limit to the proliferation rate. The normal turnover rate of endothelial cells is negligible on the time-scale that we are considering [8]. In normal endothelium, the labelling index was found to be as low as 0.01% per hour in some cases (Denekamp (1984)). The proliferation of capillary vessels is initiated by the release of TAF and so is dependent on the density of tumour cells n_1. We take the vessel proliferation term to be $\dfrac{Sn_1n_2}{\beta + n_2}$.

In this model we assume that the main cause of tumour cell death is due to nutrient deficiency [16]. Capillary vessels may fail to reach some parts of the tumour or tumour cell overcrowding and high internal pressure may cause vessels to collapse [16], [17]. If the oxygen concentration in a tumour cell is inadequate for normal cell functions, the cell becomes hypoxic which leads to a reduction in cell activity. A hypoxic cell can return to normal if nutrient levels increase but will eventually die if deprived of oxygen for too long. In this model we assume that once a cell has become hypoxic it will subsequently die. In the discussion we will suggest a way of incorporating temporarily hypoxic tumour cells into a model. Let N_2 be some reference vessel surface area such as the surface area per unit volume at the point of vascularization. We choose $\alpha n_1(1-\tanh((n_2-N_2)/N_2))$ as our tumour cell death term as this gives us a smooth switch from high to low death as n_2 increases. Furthermore, there is a finite limit to tumour cell death as $n_2 \to 0$, which suggests that the tumour returns to its dormant state as nutrients decrease (figure(1(a))).

The death of vasculature is mainly due to overcrowding of vessels and tumour cells. We would expect a sharp increase in vessel death as n_2 increases and also a term which depended on n_1. We chose $\dfrac{An_1n_2^2}{B+n_2^2}$ as our vessel death term. This term has previously been used to describe spruce budworm death due to overcrowding and predation [18]. In a similar manner tumour cells invade the blood vessels which collapse due to the massive increase in tumour volume (figure(1(b))).

In the model, we assume that all growth is in the radial direction only and we have radial symmetry. If R is the distance from the centre of the tumour we have the system

$$\begin{aligned}
\frac{\partial n_1}{\partial t} &= \frac{D_1}{R^2}\frac{\partial}{\partial R}\left(R^2\frac{\partial n_1}{\partial R}\right) - \frac{1}{R^2}\frac{\partial}{\partial R}\left(R^2\chi n_1\frac{\partial n_2}{\partial R}\right) \\
&\quad + rn_1n_2 - \alpha n_1\left(1-\tanh\frac{(n_2-N_2)}{N_2}\right), \qquad (1)\\
\frac{\partial n_2}{\partial t} &= \frac{D_2}{R^2}\frac{\partial}{\partial R}\left(R^2\frac{\partial n_2}{\partial R}\right) + \frac{Sn_1n_2}{\beta+n_2} - \frac{An_1n_2^2}{B+n_2^2}. \qquad (2)
\end{aligned}$$

Let L be some reference length such as the distance from the tumour boundary to the parent vessel, let $\tau = L^2/D_2$ be our reference time and N_1 a reference tumour cell density. By making the following substitutions;

$$n_1^* = \frac{n_1}{N_1},\ n_2^* = \frac{n_2}{N_2},\ R^* = \frac{R}{L},\ t^* = \frac{t}{\tau},$$

$$D = \frac{D_1}{D_2},\ \chi^* = \frac{\chi N_2}{D_2},\ r^* = rN_2\tau,\ \alpha^* = \alpha\tau,$$

$$\beta^* = \frac{\beta}{N_2},\ B^* = \frac{B}{N_2^2},\ A^* = \frac{AN_1\tau}{N_2},\ S^* = \frac{SN_1\tau}{N_2},$$

and dropping the asterisks for notational convenience, we obtain the dimensionless system

$$\frac{\partial n_1}{\partial t} = \frac{D}{R^2}\frac{\partial}{\partial R}\left(R^2\frac{\partial n_1}{\partial R}\right) - \frac{1}{R^2}\frac{\partial}{\partial R}\left(R^2\chi n_1\frac{\partial n_2}{\partial R}\right) + rn_1n_2 - \alpha n_1\left(1-\tanh(n_2-1)\right), \tag{3}$$

$$\frac{\partial n_2}{\partial t} = \frac{1}{R^2}\frac{\partial}{\partial R}\left(R^2\frac{\partial n_2}{\partial R}\right) + \frac{Sn_1n_2}{\beta+n_2} - \frac{An_1n_2^2}{B+n_2^2}. \tag{4}$$

To close the system we impose the following boundary conditions;

$$\text{At } R=0,\ \frac{\partial n_1}{\partial R} = 0,\ \frac{\partial n_2}{\partial R} = 0.$$

$$\text{At } R=1,\ \frac{\partial n_1}{\partial R} = 0,\ n_2 = 1.$$

The first set of boundary conditions arises naturally from the symmetry of the system. Once the tumour cells reach the right-hand boundary the assumptions of the model will no longer hold, since other interactions become important (e.g. the invasion of the limbus by the tumour cells).

2.1 Estimation of Parameters

Whenever possible experimental data was used to estimate our parameter values. Where this was difficult, we chose parameters that reflected the qualitative behaviour of the tumour cells and the blood vessels.

A summary of data on corneal implants was given by Balding and McElwain (1984) [19]. A tumour will successfully induce angiogenesis if placed at a distance of 0.8mm [6] to 3mm [5] from the limbal vessels. The time for vascularization is approximately

8 to 12 days [10], [5], [6]. This gives a value for $D_2 \simeq 10^{-7}\mathrm{cm}^2\mathrm{s}^{-1}$ for $\tau \simeq 10$ days and $L \simeq 0.3$cm. Sherratt and Murray (1990) [20] estimated the diffusion coefficient of the cells in their model of epidermal wound healing. They used diffusion coefficients of $3 \times 10^{-9}\mathrm{cm}^2\mathrm{s}^{-1}$, $3.5 \times 10^{-10}\mathrm{cm}^2\mathrm{s}^{-1}$ and $6.9 \times 10^{-11}\mathrm{cm}^2\mathrm{s}^{-1}$. In their study of individual endothelial cells, Stokes and Lauffenburger (1991) [21] measured the motility parameters for endothelial cells . The mean random motility coefficient for endothelial cells migrating in αFGF was $7.1 \pm 2.7 \times 10^{-9}\mathrm{cm}^2\mathrm{s}^{-1}$. A reasonable estimate of the diffusion coefficient of tumour cells would be in the range 10^{-9} to $10^{-11}\mathrm{cm}^2\mathrm{s}^{-1}$. This would give a range for D of 10^{-4} to 10^{-2}. We would expect the diffusion of tumour cells to be small in comparison with the directed movement of the tumour cells up a gradient of blood vessels. We chose the taxis coefficient to be ten times that of the tumour cell diffusion so that for $N_2 = 10^3$, an approximate range for χ is 1 to 100. The parameter r corresponds to the tumour proliferation rate which we would expect to be fairly high. If tumour cell proliferation was about 0.1% per hour then $r \sim O(10^2)$. α represents the maximum death rate in the absence of capillary vessels. Denekamp (1984) stated that the lifespan of a nutrient-deprived hypoxic cell is 5 to 10 hours. The proportion of hypoxic cells in a tumour can be up to 80% . Hence a reasonable range for α is 1–20. For the capillary vessels, the parameters S and A represent the maximum proliferation and death rates respectively, whereas β and B are measures of the critical value at which proliferation or death is switched on. A low value of β or B means a low threshold. The tumour's vasculature is highly vulnerable [16], [8] and hence we chose a low death threshold value, $B = 0.01$, and a high maximum death rate, $A = 100$, in comparison to the proliferation threshold, $\beta = 1$, and the maximum proliferation rate $S = 10$.

2.2 Numerical Simulations

The system of equations were solved using a routine available from the NAG library which integrates the system using the method of lines and Gear's method. Three different sets of initial conditions were used (figure (2)).

In the first case, we tried similar initial conditions to those used by Liotta et al. (1977) [22] in their model of tumour vascular growth, i.e. unit step functions (figure (2a)). Assuming that the tumour is placed at a distance of 3mm from the parent vessel and that its radius is about 1mm, we take the tumour boundary to be at $R = 0.25$. The results are given in figure (3). A peak of tumour cells moves across the domain towards the parent vessel and there is a decline in tumour density at the centre, indicating that a necrotic core has developed. The capillary vessels have infiltrated the tumour mass and they have slightly regressed from the advancing front of tumour cells. However, the vessels have not degenerated at the centre of the tumour as expected.

In the second case, a more realistic initial profile for the tumour cells was chosen and we chose a Gaussian distribution of cells centred at $R = 0.2$ (figure (2b)). This corresponds to a newly vascularized tumour nodule with central necrosis surrounded by a layer of live proliferating cells. Again, the results show (figure (4)) a peak of advancing tumour cells penetrated by capillaries. The regression of vessels is slightly more pronounced and after time $t = 0.03$ the density of vessels at the centre of the tumour begins to decrease.

Finally, we took an initial profile of capillary vessels from a model of angiogenesis by Chaplain and Stuart (1993) [23] (figure (2c)). The taxis coefficient χ is reduced in order to allow more time for the overcrowding to take effect and also the tumour cell proliferation rate r was increased. Figure (5) shows an advancing peak of tumour cells and a substantial increase in tumour cell density with time. The capillaries have penetrated the tumour mass but have collapsed at the centre and the vasculature has regressed considerably.

We note that the qualitative form of the numerical solutions are wave-like. Hence in the next section we will investigate the possibility of travelling wave solutions with constant speed and profile.

3 Travelling Wave Analysis

In this section, we will conduct a travelling wave analysis by considering the system of partial differential equations (3)–(4) in one space dimension. We will approximate the original model by replacing the proliferation term for the blood vessels by the logistic growth term $Sn_2(1-n_2)$, where the parameters are dimensionless. The use of this term can be justified by assuming that the blood vessels have been saturated by TAF and hence the proliferation of vessels is independent of tumour cell density. Hence our model in Cartesian co-ordinates becomes

$$\begin{aligned}
\frac{\partial n_1}{\partial t} &= D\frac{\partial^2 n_1}{\partial R^2} - \chi\frac{\partial}{\partial R}\left(n_1\frac{\partial n_2}{\partial R}\right) + rn_1n_2 - \alpha n_1(1-\tanh(n_2-1)), &(5)\\
\frac{\partial n_2}{\partial t} &= \frac{\partial^2 n_2}{\partial R^2} + Sn_2(1-n_2) - \frac{An_1n_2^2}{B+n_2^2}. &(6)
\end{aligned}$$

The spatially homogeneous steady states are given by $(0,0)$, $(0,1)$ and $(n_1^\star, n_2^\star)$ where

$$n_1^\star = \frac{S(1-n_2^\star)(B+n_2^{\star 2})}{An_2^\star}, \tag{7}$$

and $n_2^\star$ uniquely satisfies

$$rn_2^\star - \alpha(1-\tanh(n_2^\star - 1)) = 0. \tag{8}$$

We look for solutions of the form $N_1(z) = n_1(R,t)$, $N_2(z) = n_2(R,t)$, where $z = R - ct$, c

is a constant positive wave speed, so that the waves travel to the right. Using the notation $'$ to denote differentiation with respect to z, we obtain a fourth order system of ordinary differential equations

$$-cN_1' = DN_1'' - \chi(N_1 N_2')' + rN_1N_2 - \alpha N_1(1 - \tanh(N_2 - 1)), \tag{9}$$

$$-cN_2' = N_2'' + SN_2(1 - N_2) - \frac{AN_1N_2^2}{B + N_2^2}. \tag{10}$$

The boundary conditions are given below, i.e. non-negative solutions satisfying

$$\begin{aligned} N_1(-\infty) &= n_1^\star,\ N_1(+\infty) &&= 0, \\ N_2(-\infty) &= n_2^\star,\ N_2(+\infty) &&= 1, \\ N_1'(\pm\infty) &= 0,\ N_2'(\pm\infty) &&= 0. \end{aligned} \tag{11}$$

Waves satisfying (11) can be described as 'waves of invasion'. In this case, we have one population at its carrying capacity. Introducing a small amount of another species, the system evolves to a new steady state of co-existence where the original population has decreased and the new species has increased. From this description of invasion, we infer $n_2^\star < 1$. In the biological situation that we are considering, tumour cells invade a population of endothelial cells.

We will analyse the system (9) and (10) by considering two cases. First, we will simplify the system by setting $D = 0$, which is the limiting case of D small. In this case the vessels are diffusing much faster than the tumour cells. This implies that there is little random motion of tumour cells, therefore the emphasis is on the directed movement of tumour cells into the capillary vessels. Next, we will consider D non zero.

3.1 Case 1: $D = 0$.

Let $W = N_2'$, then we obtain the following three-dimensional phase space:

$$\begin{aligned} N_1' &= \left(\frac{1}{\chi W - c}\right)[rN_1N_2 - \alpha N_1(1 - \tanh(N_2 - 1)) \\ &\qquad + \chi N_1(SN_2(1 - N_2) - \frac{AN_1N_2^2}{B + N_2^2} + cW)], \qquad (12) \\ N_2' &= W, \qquad (13) \\ W' &= \frac{AN_1N_2^2}{B + N_2^2} - SN_2(1 - N_2) - cW. \qquad (14) \end{aligned}$$

To remove the singularity at $W = \frac{c}{\chi}$, let $(\chi W - c)\frac{d}{dz} = \frac{d}{d\xi}$. Hence we obtain the following system:

$$\begin{aligned} \frac{dN_1}{d\xi} &= rN_1N_2 - \alpha N_1(1 - \tanh(N_2 - 1)) \\ &\qquad + \chi N_1(SN_2(1 - N_2) - \frac{AN_1N_2^2}{B + N_2^2} + cW), \qquad (15) \\ \frac{dN_2}{d\xi} &= W(\chi W - c) \qquad (16) \\ \frac{dW}{d\xi} &= (\frac{AN_1N_2^2}{B + N_2^2} - SN_2(1 - N_2) - cW)(\chi W - c). \qquad (17) \end{aligned}$$

We will carry out a phase plane analysis in the usual way by linearizing about each critical point to obtain a system of the form

$$\frac{d\mathbf{X}}{d\xi} = A\mathbf{X}, \quad \text{where } \mathbf{X} = (N_1, N_2, W)^T$$

and A is a 3×3 Jacobian matrix which has been evaluated at the critical point. The eigenvalues are then given by $\det(A - \lambda I)$=0. Using the notation A_{ij} to denote the element in the i^{th} row and j^{th} column of the matrix A, we obtain

$$\lambda^3 - \lambda^2(A_{11} + A_{33}) + \lambda(A_{11}A_{33} - A_{13}A_{31} - A_{23}A_{32}) + A_{11}A_{23}A_{32} - A_{12}A_{23}A_{31} = 0. \quad (18)$$

since A_{21} and A_{22} are always zero when evaluated at any of the critical points. The analysis of this phase space is given in the appendix. A summary of the results are as follows.

- The critical point (0,0,0) is a stable node if $c^2 < \alpha(1 + \tanh 1) < S$. Otherwise, the critical point is a saddle point.
- For non-negative solutions passing through (0,0,0), the parameters must satisfy equations (27) and (28) as given in the appendix.
- Since $r > \alpha$ from equation (8), the critical point (0,1,0) is a saddle.
- For non-negative solutions passing through (0,1,0), the parameters must satisfy equations (30) and (31).
- The critical point $(n_1^\star, n_2^\star, 0)$ is a stable node if $c^2 < \chi S n_2^\star(1 - n_2^\star)$, otherwise it is a saddle.

We solved the three dimensional system of equations (15)-(17) using an ODE solver implemented in MATLAB with the parameters $D = 0$, $\chi = 10$, $r = 100$, $\alpha = 10$, $S = 10$, $\beta = 1$, $A = 100$, $B = 0.01$ and the wavespeed $c = 16.9$ which was derived from conditions (30) and (31). This compares well to the wavespeed of $c = 15$ which was found by examining the numerical solutions of the original PDE's. Using the parameter estimates $L \simeq 0.3$cm as a reference length and $\tau \simeq 10$ days as a reference time, we estimate the speed of invasion to be $6 \times 10^{-6}\text{cms}^{-1}$.

Figures (6) and (7) show the profiles of the wave front for the tumour cell density and the vessel density respectively. It may be possible to obtain a numerical solution of the complete wave profile by using a shooting method which is specially tailored to this problem. However we do not explore that avenue here since the problem is non-standard and will be dealt with in a separate paper.

3.2 Case 2: $D > 0$

Let $U = N_1'$ and $V = N_2'$. Then we have a four dimensional phase space,

$$\begin{aligned}
N_1' &= U, && (19)\\
N_2' &= V, && (20)\\
U' &= \frac{1}{D}[\chi(UV + N_1(\frac{AN_1N_2^2}{B+N_2^2} - SN_2(1-N_2) - cV))\\
&+ \alpha N_1(1-\tanh(N_2-1)) - rN_1N_2 - cU], && (21)\\
V' &= \frac{AN_1N_2^2}{B+N_2^2} - SN_2(1-N_2) - cV. && (22)
\end{aligned}$$

We will carry out a phase plane analysis in the usual way by linearizing about each critical point to obtain a system of the form

$$\frac{d\mathbf{X}}{dz} = A\mathbf{X}, \quad \text{where } \mathbf{X} = (N_1, N_2, U, V)^T$$

and A is a 4×4 Jacobian matrix which has been evaluated at the critical point. The eigenvalues are then given by $\det(A - \lambda I)=0$. Using the notation A_{ij} to denote the element in the i^{th} row and j^{th} column of the matrix A, we obtain

$$\lambda^4 \quad + \quad \lambda^3(c - A_{33}) - \lambda^2(A_{42} + A_{31} + cA_{33})$$

$$+ \quad \lambda(A_{33}A_{42} - cA_{31} - A_{34}A_{41}) + A_{31}A_{42} - A_{32}A_{41} = 0. \tag{23}$$

The analysis of this phase space is given in the appendix. A summary of the results are as follows.

- The condition $S < \alpha(1+\tanh 1)$ is sufficient to ensure that the critical point (0,0,0,0) has an unstable manifold.
- The critical point (0,1,0,0) is a saddle since $r > \alpha$.
- The critical point $(n_1^\star, n_2^\star, 0, 0)$ is a stable node if $\frac{1}{27} > B > 0$ and $c^2 < \chi S n_2^\star(1 - n_2^\star)$, otherwise it is a saddle.

Again, we solved the system of equations (19)–(22) using MATLAB with the parameters $D = 0.01$, $\chi = 10$, $r = 100$, $\alpha = 10$, $S = 10$, $\beta = 1$, $A = 100$, $B = 0.01$ and the wavespeed $c = 15$ which was measured from the original numerical solutions of the PDE's. Figures (8) and (9) show the profiles of the wave front for the tumour cell density and the vessel density respectively.

4 Discussion

This model has captured the key initial events of vascular tumour growth such as the migrating front of tumour cells, necrosis and the regression of blood vessels. The advance of tumour cells across the host-tissue field is attributed to a combination of diffusion, active migration and proliferation of tumour cells. Liotta et al. (1977) explains central necrosis as a failure of new blood vessels to reach the centre of the tumour fast enough. However, shortly after vascularization, the whole of the tumour is criss-crossed by capillaries [8], with necrosis reappearing later. Hence, in this model the development of a necrotic core is due to overcrowding and the eventual collapse of the blood vessels.

It is encouraging that the results improve as the initial conditions are made more realistic. Nevertheless, the model neglects many other features of tumour growth. We do not consider the effect of extravascular pressure or the compression of host tissue which can obstruct the flow of blood to the tumour cells [4]. Denekamp (1984) reports on the possibility of cyclic hypoxia, that is the temporary opening and closing of vessels for a few seconds or even for a few hours. We could model the effects of cell-matrix interactions by developing a mechanical model [18]. Alternatively, we could include temporarily and permanently hypoxic cells by developing an age-structured model. This would involve two age classes for the tumour cells with 'young' proliferating cells in one class and 'old' reduced activity cells in the other, with cells switching from class to class whenever nutrient levels were above or below some threshold value.

In our model, we assumed radial symmetry. It is unusual for tumours to grow outward to an equal extent in all directions except when grown in a homogeneous enviroment, e.g. in the liver. Studies on multicellular spheriods [24] have shown that there is heterogeneity in both the cells and the enviroment. It may be possible to capture this feature by producing models in two or three dimensions, or by assuming non-linear diffusion.

References

[1] D. Darling and D. Tarin. The spread of cancer in the human body. *New Scientist*, pages 50–53, July 1990.

[2] L. Edelstein-Keshet. *Mathematical Models in Biology*. Random House, 1988.

[3] M. LaBarbera and S. Vogel. The design of fluid transport systems in organisms. *American Scientist*, **70**:54–60, 1982.

[4] J. Folkman. Tumor angiogenesis. *Adv. Cancer Res.*, **43**:175–203, 1985.

[5] M. A. Gimbrone, R. S. Cotran, S. B. Leapman, and J. Folkman. Tumor growth and neovascularization: An experimental model using the rabbit cornea. *J. Natl. Cancer Inst.*, **52**(2):413–427, 1974.

[6] V. R. Muthukkaruppan, L. Kubai, and R. Auerbach. Tumor-induced neovascularization in the mouse eye. *J. Natl. Cancer Inst.*, **69**:699–704, 1982.

[7] M. E. Maragoudakis, P. Gullino, and P. I. Lelkes, editors. *Angiogenesis in Health and Disease*. Plenum Press, New York, 1992.

[8] N. Paweletz and M. Knierim. Tumor related angiogenesis. *Crit. Rev. Oncol. Hematol.*, **9**:197–242, 1989.

[9] J. Folkman and M. Klagsbrun. Angiogenic factors. *Science*, **235**:442–447, 1987.

[10] D. H. Ausprunk and J. Folkman. Migration and proliferation of endothelial cells in preformed and newly formed blood vessels during tumor angiogenesis. *Microvasc. Res.*, **14**:53–65, 1977.

[11] C. H. Blood and B. R. Zetter. Tumor interactions with the vasculature: angiogenesis and tumor metastasis. *Biochim. Biophys. Acta*, **1032**:89–118, 1990.

[12] J. Folkman and C. Haudenschild. Angiogenesis in vitro. *Nature*, **288**:551–556, 1980.

[13] R. Langer, H. Brem, K. Falterman, M. Klein, and J. Folkman. Isolation of a cartilage factor that inhibits tumor neovascularization. *Science*, **193**:70–72, 1976.

[14] J. A. Adam and S. A. Maggelakis. Diffusion regulated growth characteristics of a spherical prevascular carcinoma. *Bull. Math. Biol.*, **52**(4):549–582, 1990.

[15] H.P. Greenspan. Models for the growth of a solid tumor by diffusion. *Stud. Appl. Math.*, **51**:317–340, 1972.

[16] J. Denekamp. Vascular endothelium as the vulnerable element in tumours. *Acta Radiol. Oncol.*, **23**:217–225, 1984.

[17] R. K. Jain. Barriers to drug delivery in solid tumors. *Sci. Am.*, **271**(1):58–65, 1994.

[18] J. D. Murray. *Mathematical Biology.* Springer-Verlag, Berlin, 1989.

[19] D. Balding and D. L. S. McElwain. A mathematical model of tumour induced capillary growth. *J. Theor. Biol.*, **114**:53–73, 1985.

[20] J. A. Sherratt and J. D. Murray. Models of epidermal wound healing. *Proc. R. Soc. Lond. B*, **241**:29–36, 1990.

[21] C. L. Stokes, D. A. Lauffenburger, and S. K. Williams. Migration of individual microvessel endothelial cells: stochastic model and parameter measurement. *J. Cell. Sci.*, **99**:419–430, 1991.

[22] L.A. Liotta, G. M. Saidel, and J. Kleinerman. Diffusion model of tumor vascularization and growth. *Bull. Math. Biol.*, **39**:117–128, 1977.

[23] M. A. J. Chaplain and A. M. Stuart. A model mechanism for the chemotactic response of endothelial cells to tumour angiogenesis factor. *IMA J. Math. Appl. Med. Biol.*, **10**:149–168, 1993.

[24] R. M. Sutherland. Cell and enviroment interaction in tumor microregions: the multicell spheriod model. *Science*, **240**:177–184, 1988.

5 Appendix A: Analysis of the three dimensional phase space

5.1 At the critical point (0,0,0)

$$A_{11} = -\alpha(1+\tanh 1), \quad A_{12} = 0, \quad A_{13} = 0, \quad A_{23} = -c,$$
$$A_{31} = 0, \quad A_{32} = Sc, \quad A_{33} = c^2.$$

Hence the eigenvalues are given by the roots of

$$p(\lambda) = \lambda^3 + \lambda^2 a_1 + \lambda a_2 + a_3, \tag{24}$$

where

$$a_1 = \alpha(1+\tanh 1) - c^2,$$

$$a_2 = c^2(S - \alpha(1+\tanh 1)),$$

$$a_3 = Sc^2\alpha(1+\tanh 1).$$

If $c^2 < \alpha(1+\tanh 1) < S$ then the origin is a stable node. Otherwise, the critical point is a saddle point.

For non-negative solutions, we require these roots to be real. We must impose the conditions $\alpha_1 > 0$ and $\beta_1 = 0$ (Murray (1989)) where

$$\alpha_1 = \left(\frac{a_1}{3}\right)^2 - \left(\frac{a_2}{3}\right), \tag{25}$$
$$\beta_1 = 2\left(\frac{a_1}{3}\right)^3 - \frac{a_1 a_2}{3} + a_3. \tag{26}$$

From the first condition we have

$$\alpha^2(1+\tanh 1)^2 + c^4 - 3c^2S + c^2\alpha(1+\tanh 1) > 0. \tag{27}$$

A sufficient condition to satisfy $\alpha_1 > 0$ is $c^2 > 3S$ or $\alpha(1+\tanh 1) > 3S$.

From the second condition $\beta_1 = 0$, we have

$$\begin{aligned} 2(\alpha(1+\tanh 1))^3 + 3(\alpha(1 \ + \ \tanh 1))^2(3-2c^2) \\ +3\alpha(1+\tanh 1)(2c^4 \ + \ 3(3S-1)c^2 - 3S) + c^2(9S-2c^4) = 0. \end{aligned} \tag{28}$$

Since α is real and positive, as a minimum requirement, we need the above polynomial to have one positive root. By Descartes Rule of Signs we require

$$3 > 2c^2, \ \ 2c^4 + 3(3S-1)c^2 - 3S > 0, \ \ 2c^4 > 9S.$$

From the second condition for c^2 real and positive we must have $3S < 1$. Hence combining these conditions $\dfrac{3}{2} > c^2 > \sqrt{\dfrac{3}{2}}$ is sufficient for α real and positive.

5.2 At the critical point (0,1,0)

$$\begin{aligned} &A_{11} = r - \alpha, \quad A_{12} = 0, \qquad A_{13} = 0, \quad A_{23} = -c, \\ &A_{31} = \tfrac{-A}{B+1}, \quad A_{32} = -Sc, \quad A_{33} = c^2. \end{aligned}$$

Hence the eigenvalues are given by

$$\lambda^3 + \lambda^2(\alpha - r - c^2) + \lambda c^2(r - \alpha - S) + Sc^2(r-\alpha) = 0. \tag{29}$$

i.e. the roots of $p(\lambda) = \lambda^3 + \lambda^2 a_1 + \lambda a_2 + a_3$, where

$$a_1 = \alpha - r - c^2,$$

$$a_2 = c^2(r - \alpha - S),$$

$$a_3 = Sc^2(r - \alpha).$$

(0,1,0) is a saddle point. If $r > \alpha$, the polynomial $p(\lambda)$ will have two positive roots and one negative root. If $\alpha > r$ we will have one positive root and two negative roots. However by examination of equation (8) combined with the condition for invasion $n_2^\star < 1$, we conclude that $r > \alpha$.

Again we must impose conditions on our parameters so that the solutions are non-negative, i.e. the eigenvalues must be real. From the condition $\alpha_1 > 0$ where α_1 is given by (25) we obtain

$$\alpha^2 + r^2 + c^4 + 3Sc^2 - 2r\alpha > 0. \tag{30}$$

$r > 2\alpha$ is a sufficient but not necessary condition which satisfies (30). From $\beta_1 = 0$ where β_1 is given by (26) we obtain

$$\frac{2}{27}[-(r-\alpha) - c^2]^3 - \frac{c^2}{3}[-(r-\alpha) - c^2][(r-\alpha) - S] + Sc^2(r-\alpha) = 0.$$

$$\frac{2}{27}[-(r-\alpha) - c^2]^3 - \frac{c^2}{3}[-(r-\alpha) - c^2][(r-\alpha) - S] + Sc^2(r-\alpha) = 0.$$

After some algebra this becomes

$$2(r-\alpha)^3 - 3c^2(r-\alpha)^2 - c^2(r-\alpha)(18S + 6c^2) + c^4(2c^2 + 9S) = 0. \tag{31}$$

5.3 At the third critical point $(n_1^\star, n_2^\star, 0)$

Using equations (7) and (8), the eigenvalues are given by the cubic

$$\begin{aligned}\lambda^3 + \lambda^2[\chi n_2^\star S(1-n_2^\star) - c^2] \quad &+ \quad \lambda S c^2 \left[\frac{2n_2^\star(1-n_2^\star)}{(B+n_2^{\star 2})^2}[n_2^\star - \chi(B+n_2^{\star 2})] - 1\right] \\ &+ \quad c^2 n_2^\star S(1-n_2^\star)[r + \alpha \mathrm{sech}^2(n_2^\star - 1)] = 0 \qquad (32)\end{aligned}$$

i.e. the roots of $p(\lambda) = \lambda^3 + \lambda^2 a_1 + \lambda a_2 + a_3$ where

$$a_1 = \chi n_2^\star S(1-n_2^\star) - c^2,$$

$$a_2 = S c^2 \left[\frac{2n_2^\star(1-n_2^\star)}{(B+n_2^{\star 2})^2}[n_2^\star - \chi(B+n_2^{\star 2})] - 1\right],$$

$$a_3 = c^2 n_2^\star S(1-n_2^\star)[r + \alpha \mathrm{sech}^2(n_2^\star - 1)]$$

.

There are four possible cases, all roots negative, one root positive and two negative, one negative and two positive and all roots positive.

Suppose all the roots are negative. By the Routh-Hurwitz conditions

$$a_1,\ a_2,\ a_3 > 0.$$

The condition $n_2^\star < 1$ is satisfied and we obtain a bound on the wavespeed,

$$\text{i.e. } c^2 < \chi n_2^\star S(1-n_2^\star).$$

Consider the limiting case $a_3 = 0$. Then the roots of $p(\lambda)$ are

$$\lambda = 0, \quad \lambda_{1,2} = -a_1 \pm \sqrt{a_1^2 - 4a_2},$$

The maximum λ_M and minimum λ_m are given by

$$\frac{dp}{d\lambda} = 3\lambda^2 + 2\lambda a_1 + a_2 = 0,$$

$$\Rightarrow \lambda_{m,M} = \frac{1}{3}(-a_1 \pm \sqrt{a_1^2 - 3a_2}).$$

These are independent of a_3. As a_3 increases from zero, $p(\lambda)$ has three real negative roots. There is a critical value of a_3, $a_3^\star$ say, for which two of the roots are equal where

$$a_3^\star = \frac{1}{27}\left(a_1 + 2\sqrt{a_1^2 - 3a_2}\right)\left(a_1 - \sqrt{a_1^2 - 3a_2}\right)^2. \tag{33}$$

so for $a_3 > a_3^\star$, we have only one real root and two complex roots. Hence the solutions approach the critical point in an oscillatory manner for $a_3 > a_3^\star$ and for $0 < a_3 < a_3^\star$ they are monotonic (figure (10)).

Suppose that one of the roots of $p(\lambda)$ is positive and two roots are negative. This implies that $a_3 < 0$ and so $n_2^\star > 1$ which contradicts our previous assumption. We dismiss this case on the grounds that this situation does not arise in the biological context that we are considering.

Now suppose that two of the roots are positive and one root is negative. Then $a_3 > 0$. Either of or both of a_1 and a_2 must be negative. If $a_1 < 0$, then $c^2 > \chi n_2^\star S(1 - n_2^\star)$. If

$a_2 < 0$, then we obtain the inequality

$$(2\chi - 1)n_2^{\star 4} - 2(\chi + 1)n_2^{\star 3} + 2(1 + B(\chi - 1))n_2^{\star 2} - 2\chi B n_2^\star - B^2 < 0.$$

As before in the case where all the roots were negative, there is a critical value of a_3. As a_3 increases to this critical value, the two positive real roots become equal. So for $a_3 > a_3^\star$ we have a trajectory which oscillates away from $(n_1^\star, n_2^\star)$.

Finally, if all the roots are positive we have $a_3 < 0$. Again, we dismiss this case as it is not of biological relevance.

6 Appendix B:Analysis of the four dimensional phase space

6.1 At the critical point (0,0,0,0)

$$\begin{array}{lll} A_{31} = \frac{\alpha}{D}(1 + \tanh 1), & A_{32} = 0, & A_{33} = -\frac{c}{D}, \\ A_{41} = 0, & A_{42} = -S. & \end{array}$$

Hence the eigenvalues are given by the roots of

$$p(\lambda) = \lambda^4 + \lambda^3 a_1 + \lambda^2 a_2 + \lambda a_3 + a_4,$$

where

$$a_1 = c + \frac{c}{D},$$

$$a_2 = \frac{c^2}{D} + S + \frac{\alpha}{D}(1 + \tanh 1),$$

$$a_3 = \frac{cS}{D} - \frac{\alpha c}{D}(1 + \tanh 1),$$

$$a_4 = -\frac{\alpha S}{D}(1 + \tanh 1).$$

By examination of a_3 we see that the origin is a saddle. In particular it has an unstable manifold if $S < \alpha(1 + \tanh 1)$ which agrees with the result found in appendix A.

6.2 At the critical point (0,1,0,0)

$$A_{31} = \tfrac{\alpha - r}{D}, \quad A_{32} = 0, \qquad A_{33} = -\tfrac{c}{D},$$

$$A_{34} = 0, \qquad A_{41} = \tfrac{A}{B+1}, \quad A_{42} = S.$$

Hence the eigenvalues are given by the roots of

$$p(\lambda) = \lambda^4 + \lambda^3 a_1 + \lambda^2 a_2 + \lambda a_3 + a_4,$$

where

$$a_1 = c + \frac{c}{D},$$

$$a_2 = \frac{1}{D}(c^2 + r - \alpha - DS),$$

$$a_3 = \frac{c}{D}(r - \alpha - S),$$

$$a_4 = \frac{S}{D}(\alpha - r).$$

Since $r > \alpha$, we can see that (0,1,0,0) is always a saddle.

6.3 At the critical point $(n_1^\star, n_2^\star, 0, 0)$

$$A_{31} = \frac{\chi}{D}\left(\frac{2An_1^\star n_2^\star}{B + n_2^{\star 2}} - Sn_2^\star(1 - n_2^\star)\right),$$

$$A_{32} = \frac{1}{D}(\chi A_{42} - rn_1^\star + \alpha n_1^\star \mathrm{sech}^2(n_2^\star - 1),$$

$$A_{33} = -\frac{c}{D},$$

$$A_{34} = -\frac{\chi c n_1^\star}{D},$$

$$A_{41} = \frac{A n_2^\star}{B + n_2^\star},$$

$$A_{42} = \frac{2An_1^\star n_2^\star}{B + n_2^{\star 2}}(1 - \frac{n_2^{\star 2}}{B + n_2^{\star 2}}) - S(1 - 2n_2^\star).$$

Using equations (7) and (8), the eigenvalues are given by the roots of

$$p(\lambda) = \lambda^4 + \lambda^3 a_1 + \lambda^2 a_2 + \lambda a_3 + a_4,$$

where

$$a_1 = c + \frac{c}{D},$$

$$a_2 = \frac{c^2}{D} + S\left(\left(\frac{2}{B + n_2^{\star 2}} - \frac{\chi}{D}\right) n_2^{\star 2}(1 - n_2^\star) - 1\right),$$

$$a_3 = \frac{cS}{D}\left(\frac{2n_2^{\star 2}(1 - n_2^\star)}{B + n_2^{\star 2}} - 1\right),$$

$$a_4 = \frac{\chi}{D} S n_2^\star (1 - n_2^\star)(r + \alpha \mathrm{sech}^2(n_2^\star - 1).$$

Since $n_2^\star < 1$, $a_4 > 0$. If either $a_2 < 0$ and/or $a_3 < 0$ then the critical point $(n_1^\star, n_2^\star, 0, 0)$ is a saddle. If both $a_2 > 0$ and $a_3 > 0$ then the critical point is a stable node, i.e. if

$$\frac{c^2}{D} + S\left(\left(\frac{2}{B + n_2^{\star 2}} - \frac{\chi}{D}\right) n_2^{\star 2}(1 - n_2^\star) - 1\right) > 0, \tag{34}$$

and

$$2n_2^{\star 2}(1 - n_2^\star) > B + n_2^{\star 2}. \tag{35}$$

From (35), we have $n_2^{\star 2} - 2n_2^{\star 3} > B > 0$. Consider the function $f(n_2^\star) = n_2^{\star 2} - 2n_2^{\star 3}$ for $0 < n_2^{\star 2} < 1$. Then clearly $\frac{1}{27} > B > 0$. Hence if (35) is satisfied then $c^2 > \chi S n_2^{\star 2}(1 - n_2^\star)$ is sufficient to satisfy (35).

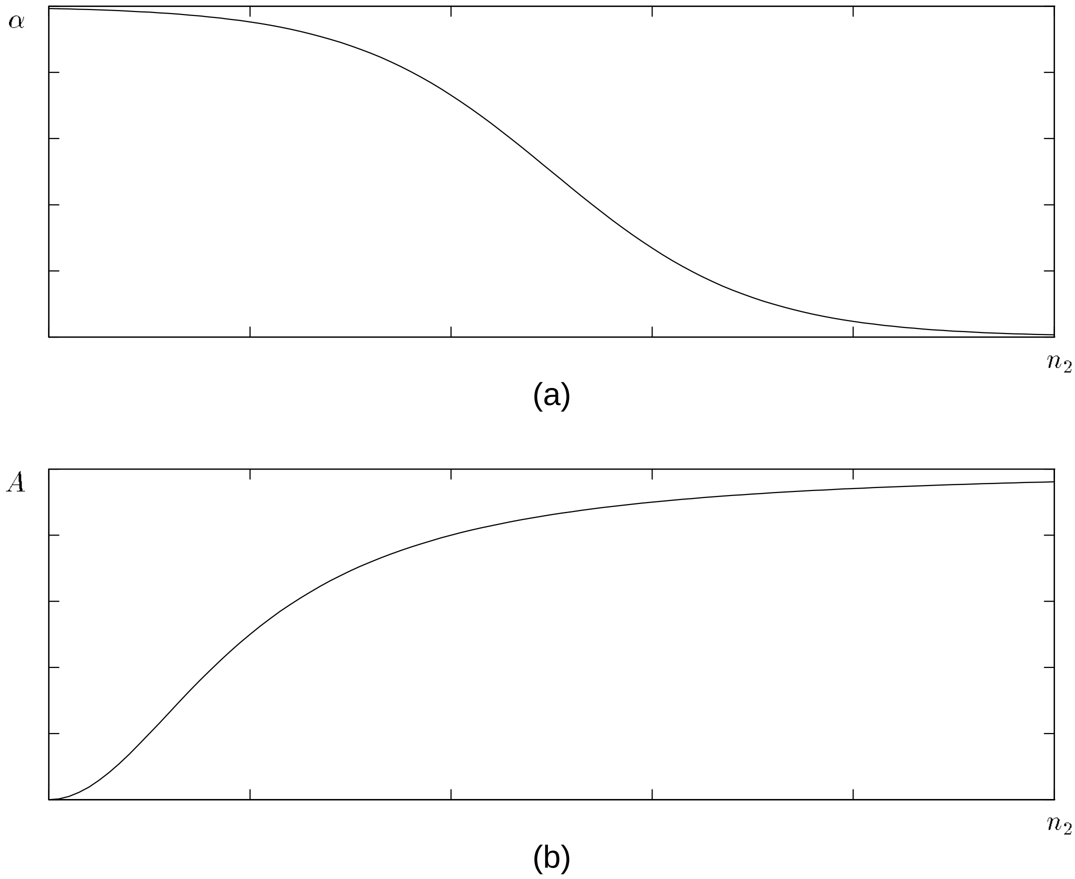

Figure 1:

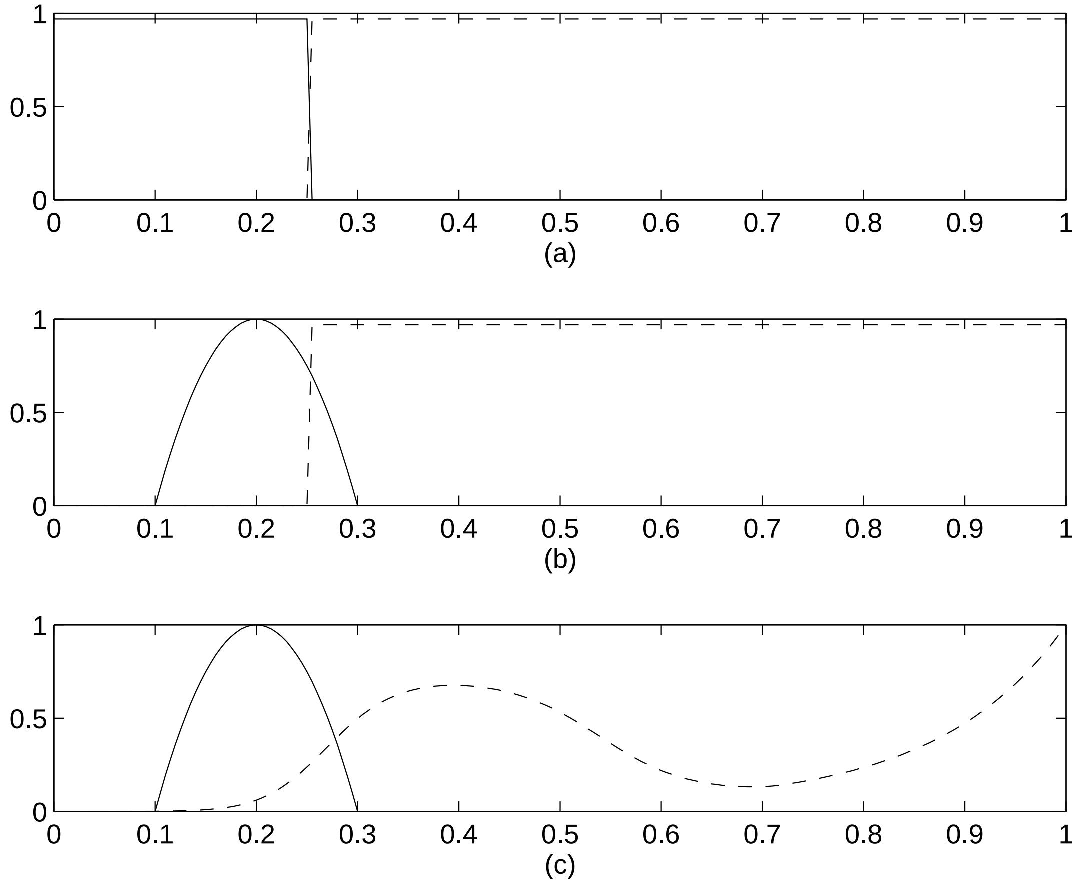

Figure 2:

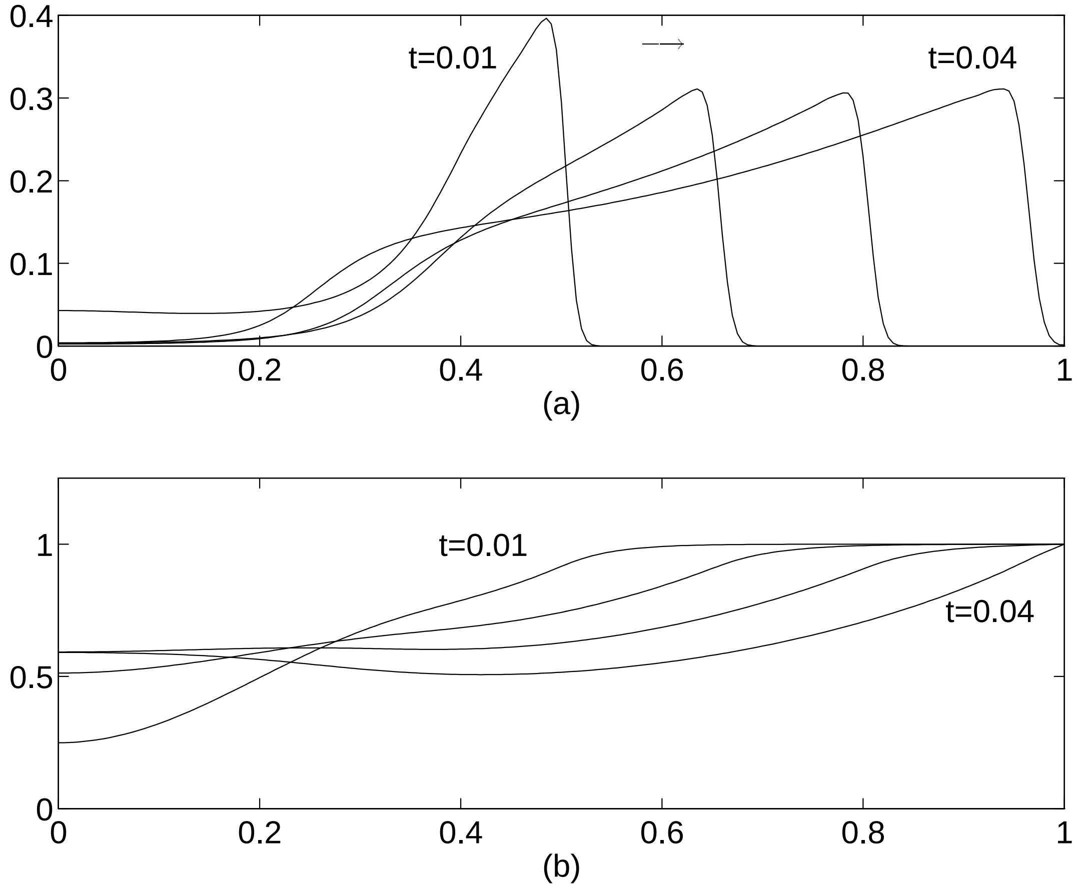

0.4
0.3
0.2
0.1
0
t=0.01
t=0.04
0
0.2
0.4
0.6
0.8
1
(a)
1
0.5
0
t=0.01
t=0.04
0
0.2
0.4
0.6
0.8
1
(b)

Figure 3:

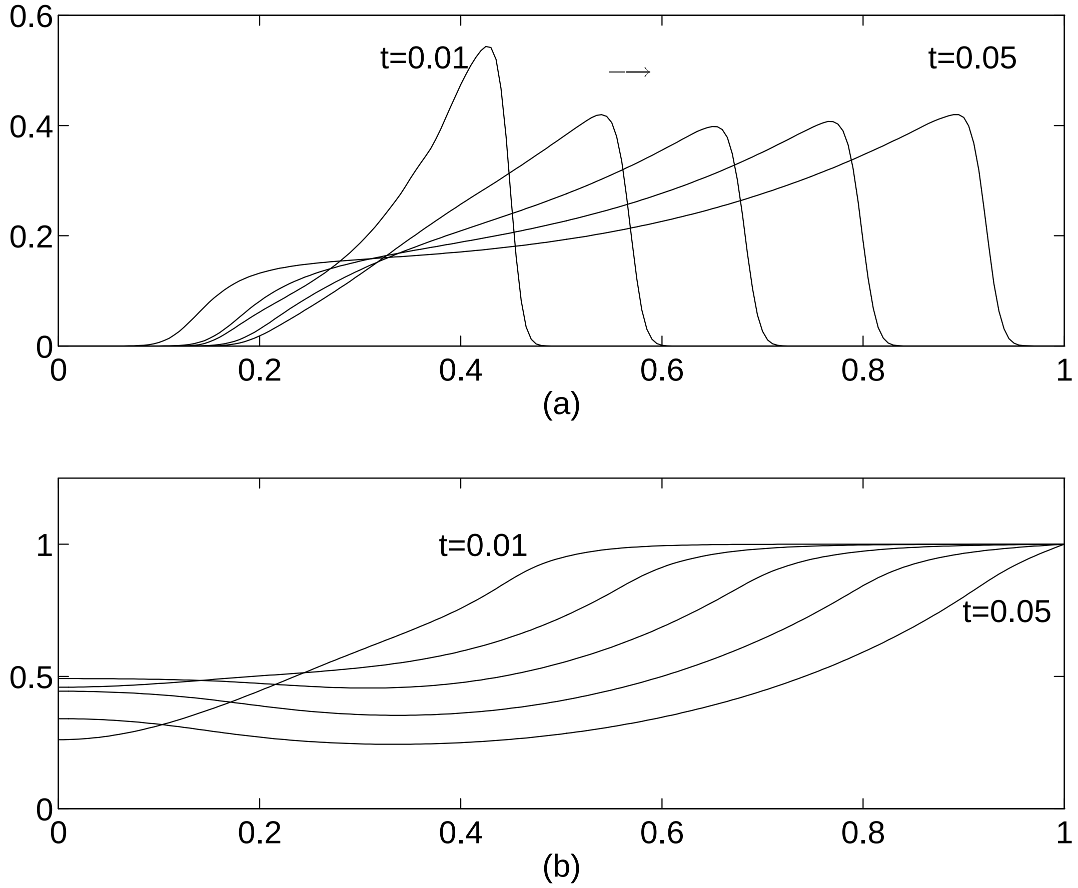

Figure 4:

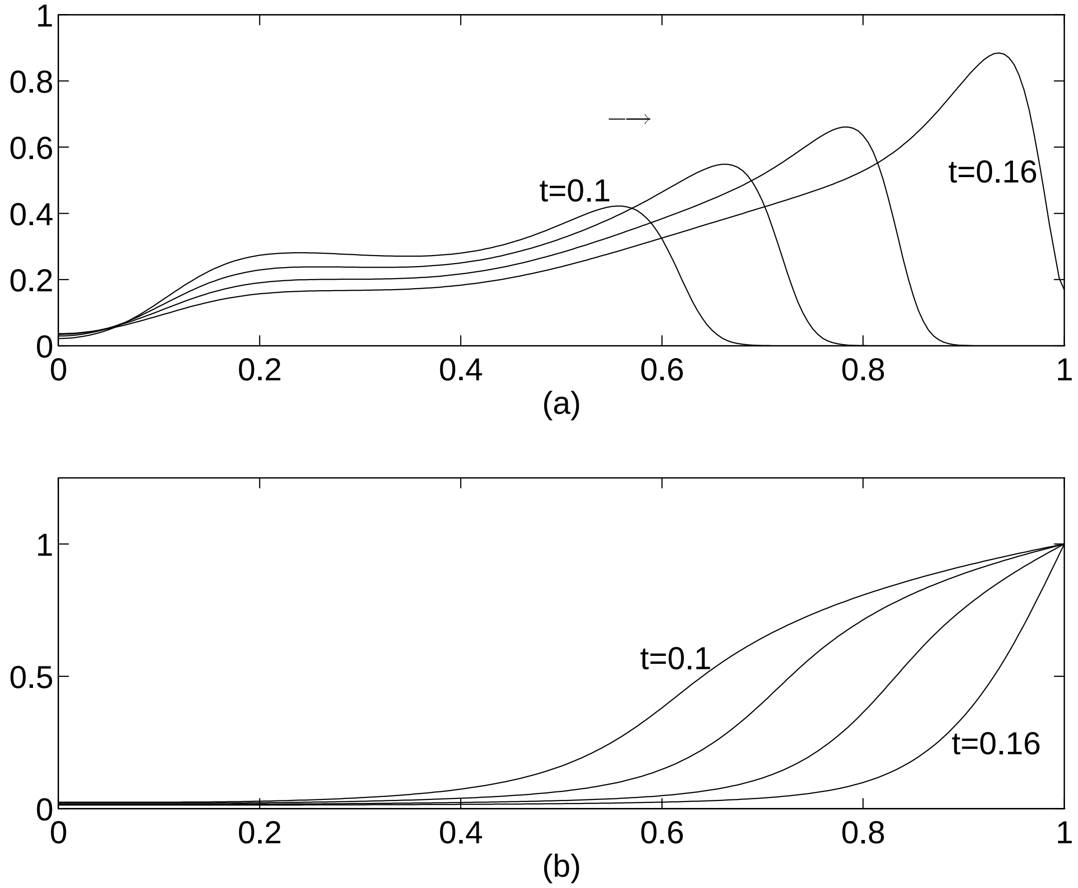

1
0.8
0.6
0.4
0.2
0
t=0.1
t=0.16
0
0.2
0.4
0.6
0.8
1
(a)
1
0.5
0
t=0.1
t=0.16
0
0.2
0.4
0.6
0.8
1
(b)

Figure 5:

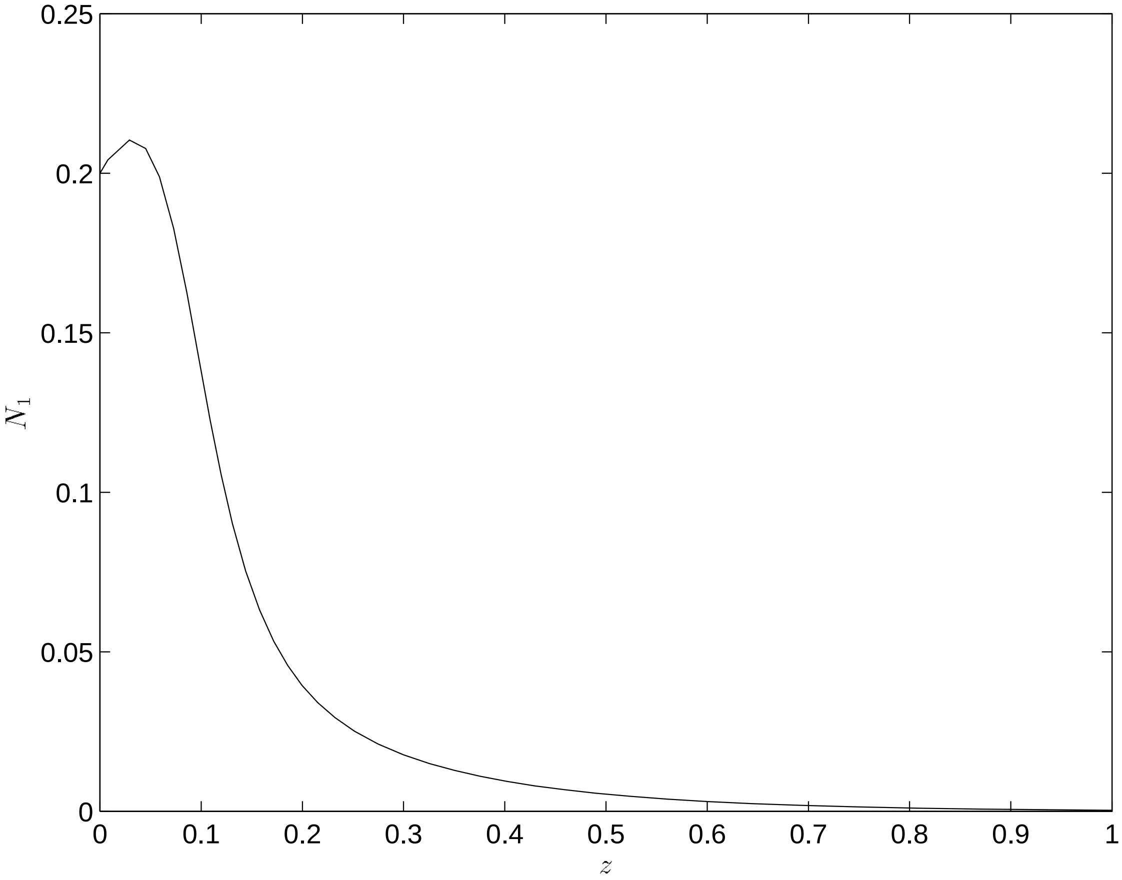

Figure 6:

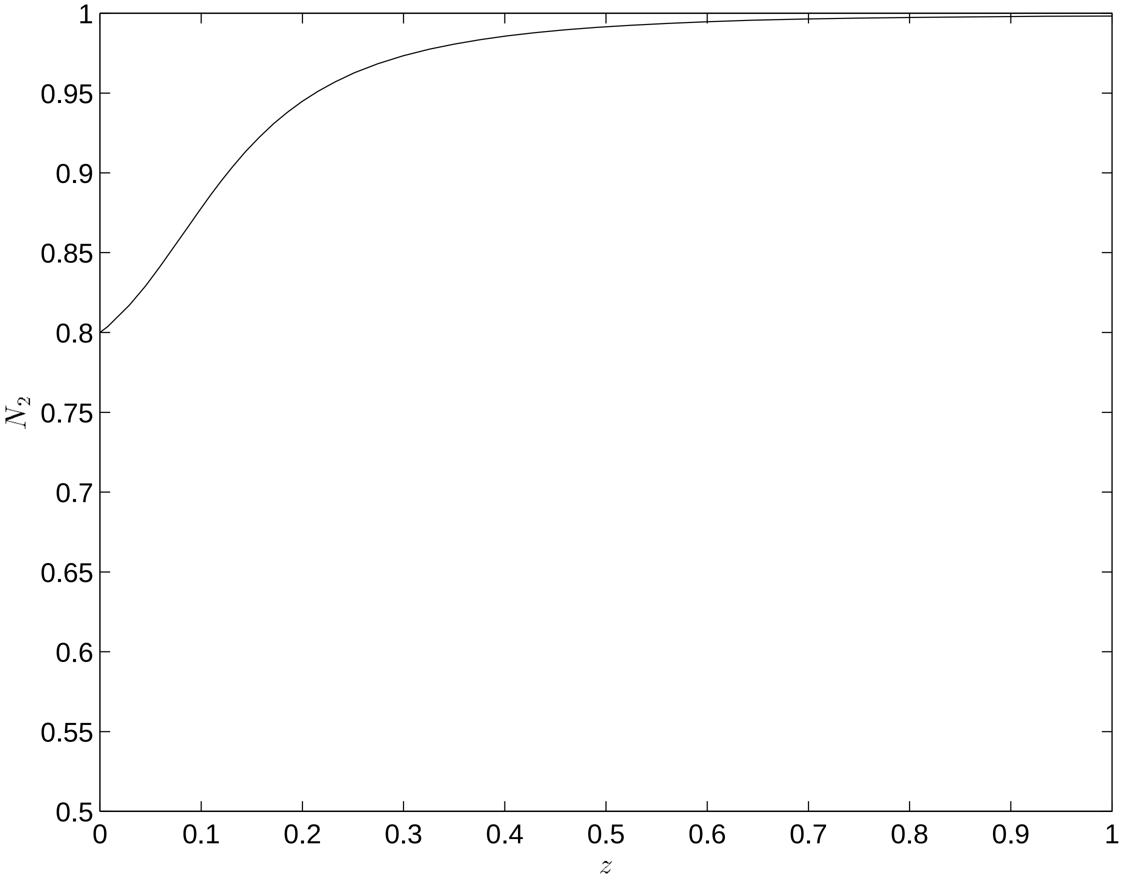

Figure 7:

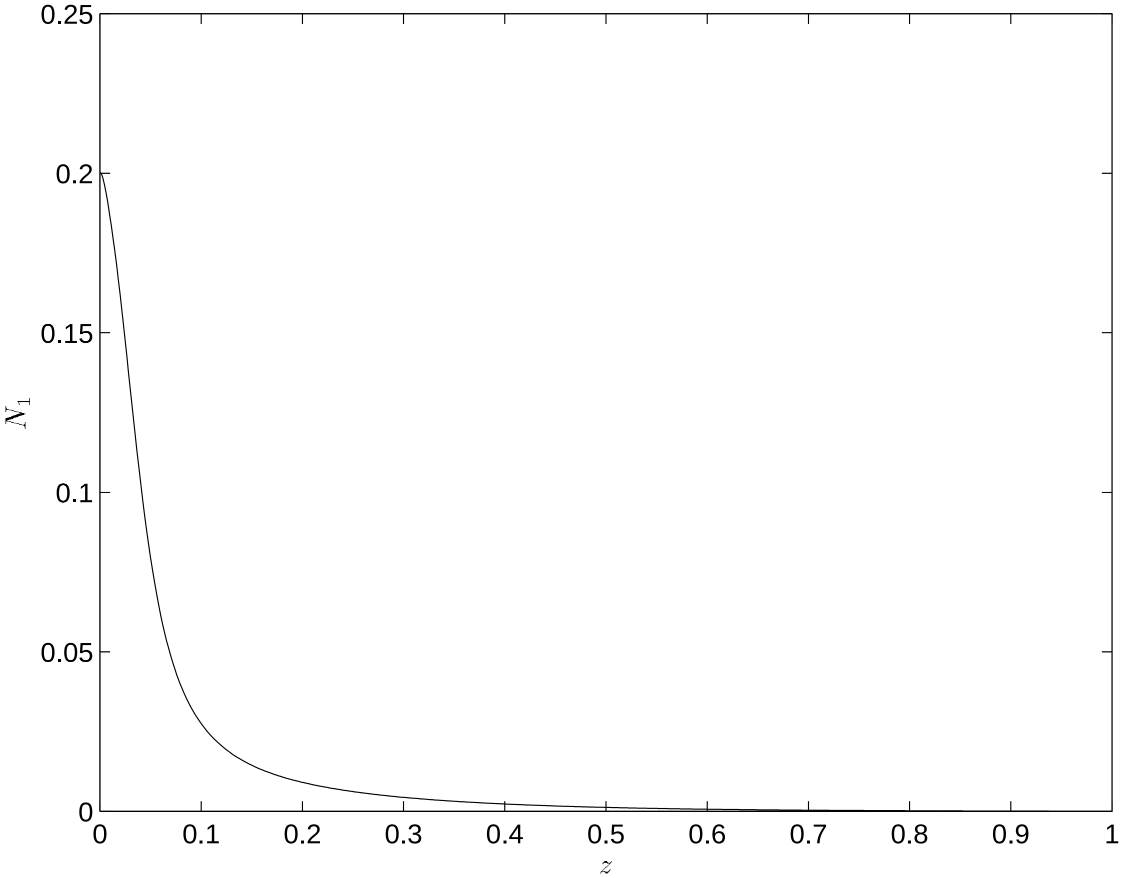

Figure 8:

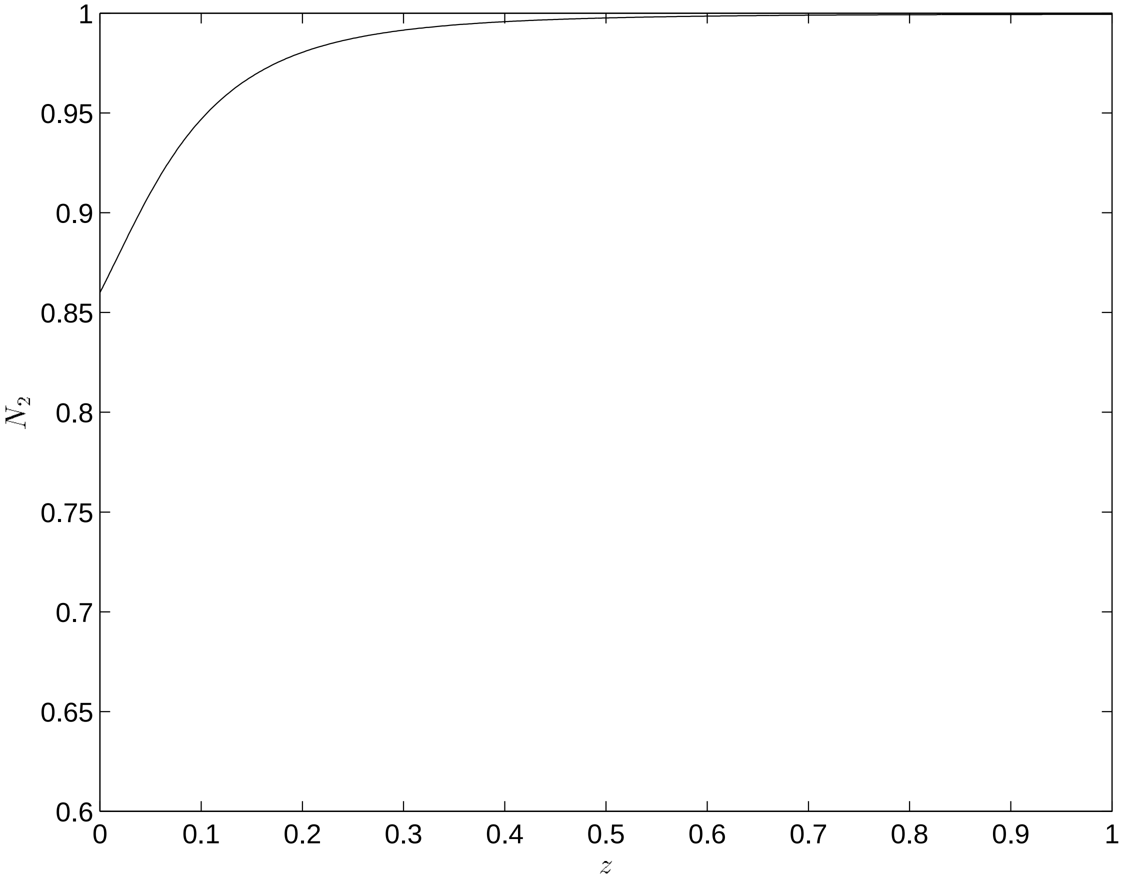

Figure 9:

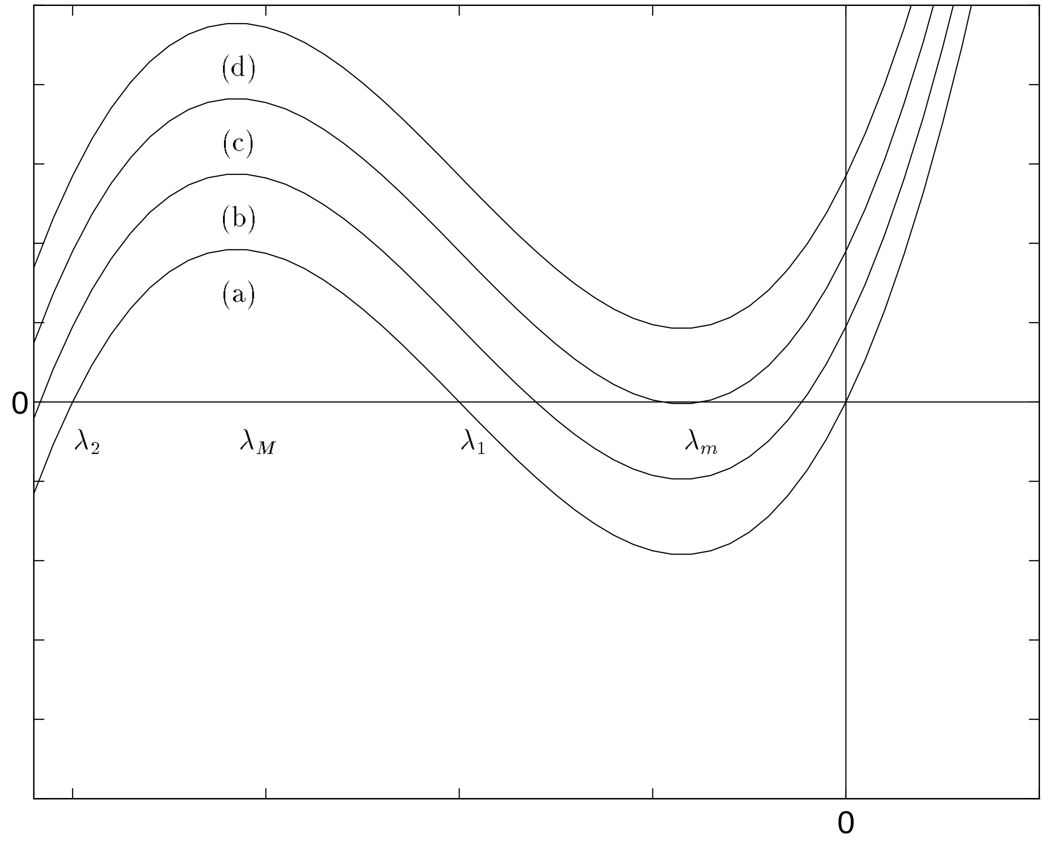

Figure 10:

Figure Legends

Figure (1): The qualitative forms of the two death terms. Figure (a) is a typical tumour cell death term $\alpha(1 - \tanh((n_2 - N_2)/N_2))$ while figure (b) shows the vessel death term $An_2^2/B + n_2^2$.

Figure (2): The three different initial conditions used to test the model. The solid line represents the tumour cell distribution and the dashed line represents the vessel density. In figure (a) we have a block distribution of tumour cells and vessels. In figure (b) we have a Gaussian distribution of tumour cells centred at 0.2. In figure (c) we have the same Gaussian distribution for the tumour cells but for the vessels we have taken a profile from the model of angiogenesis by Chaplain and Stuart (1993).

Figure (3): With block initial conditions for the tumour cells and the vessels the system evolves as shown above. Figure (a) shows the tumour cells distribution and figure (b) the vessels. Plots were taken at times $t = 0.01$, 0.02, 0.03 and 0.04. Parameters values were $D = 0.01$, $\chi = 10$, $r = 100$, $\alpha = 10$, $S = 10$, $\beta = 1$, $A = 100$, $B = 0.01$.

Figure (4): With a Gaussian distribution of tumour cells and block initial conditions for the vessels the system evolves as shown. Figure (a) shows the tumour cell density while figure (b) shows the vessel distribution. Plots were taken at times $t = 0.01$, 0.02, 0.03, 0.04 and 0.05. Parameters values were $D = 0.01$, $\chi = 5$, $r = 100$, $\alpha = 10$, $S = 10$, $\beta = 1$, $A = 100$, $B = 0.01$.

Figure (5): With an initial profile for the vessels taken from Chaplain and Stuart (1993) the system will evolve as shown. Figure (a) shows the tumour cell density while figure (b) shows the vessel distribution. Plots were taken at times $t = 0.1$, 0.12, 0.14

and 0.16. Parameters values were $D = 0.01$, $\chi = 1$, $r = 200$, $\alpha = 7$, $S = 10$, $\beta = 1$, $A = 100$, $B = 0.01$.

Figure (6): The phase space (15)-(17) was solved numerically to obtain a profile of the wave front for the tumour cell density.

Figure (7): The phase space (15)-(17) was solved numerically to obtain a profile of the wave front for the vessel density.

Figure (8): The phase space (19)-(22) was solved numerically to obtain a profile of the wave front for the tumour cell density.

Figure (9): The phase space (19)-(22) was solved numerically to obtain a profile of the wave front for the vessel density.

Figure (10): The general form of $p(\lambda)$ as a_3 increases from zero. (a) $a_3 = 0$, (b) $0 < a_3 < a_3^\star$, (c) $a_3 = a_3^\star$ and (d) $a_3 > a_3^\star$.